AN ANALYTICAL STUDY OF THE INTERACTION OF FRAMES AND INFILL MASONRY WALLS.

C. E. Rivero (I)
W. H. Walker (II)
Presenting Author: C. E. Rivero

SUMMARY

This paper presents a nonlinear dynamic model to study the behavior of frames infilled by masonry walls. The nonlinearities of the model include the interaction between the frame and wall, cracking and failure of the wall, the bracing effect that the wall has on the frame, the discontinuities between the frame and wall, and the inelastic behavior of the frame. The modeling of the masonry wall is based on the premise that the cracking mechanism of the wall may be separated from the material model assumed for the masonry. Analytical results are presented for a three story one bay frame infill with masonry walls.

INTRODUCTION

For many years infill walls have formed an integral part of buildings. Their use has been mainly as architectural elements and as such have been largely ignored by engineers when designing the main structural configuration. Engineers have normally considered these walls as brittle elements whose lateral load capacity is small when compared with the frame. This assumption ignores the confining effect that the frame has on the wall. As such there are numerous examples of frames, although properly designed to resist earthquake loading when acting alone, being severely damaged due to the presence of infill walls, acting in the plane of the frame.

In order to adequately study the interaction between the frame and the infill masonry wall under earthquake loading an analytical model was developed. This model takes into account the interaction between the frame and wall, cracking and failure of the wall, the bracing effect that the wall has on the frame and the inelastic behavior of the frame.

ANALYTICAL MODEL

The modeling of the frame-infill wall problem may be classified into two broad categories: The equivalent diagonal strut method, and the finite element method.

The equivalent diagonal strut has the great advantage of simplicity. However, the indirect provision for handling the frame-wall interaction does lack versatility, especially when nonlinear dynamic analysis is done. The finite

(I) Assistant Professor of Civil Engineering, University of Texas at Arlington, Arlington, Texas, USA.

(II) Associate Professor of Civil Engineering, University of Illinois at Urbana, Urbana, Illinois, USA.

element technique overcomes the disadvantages of the strut method. However, this is done at the expense of simplicity. The versatility gained in using finite elements is hampered by the need to use a large number of degrees of freedom to model the masonry wall. In the case of dynamic loading the number of degrees of freedom could be excessive.

The model developed in this study uses the finite element method, and as such has it's versatility; however, it reduces the number of degrees of freedom needed to model the frame-infill-wall system.

Mechanical Model

A schematic representation of the wall model as applied to a specific wall section is shown in Fig. 1. As the figure shows the modeling of the wall was divided into three areas: 1) The boundary between the frame and wall. 2) Cracking in the wall itself. 3) Uncracked behavior of the specific wall segment.

The boundary between the frame and wall was modeled by two types of elements called "gap elements" and "joint elements". The gap elements modeled the space between the frame and wall. The element kept track of gaps and determined when the frame and wall came into contact forcing continuity between the frame and wall. The joint element modeled the boundary between the frame and wall where continuity was initially assumed. This element permitted the representation of mortar joints at the base of the wall. It allowed continuity up to a certain stress then permitted change in behavior similar to the gap element.

The uncracked wall itself was represented as an assemblage of triangular elements. A joint element was placed at the edge of each wall element to approximately represent the cracking in the masonry wall. Each wall element represented several bricks and joints. It was assumed that all cracking in the wall was concentrated along the boundaries of the wall elements where the joint elements were located.

Columns and beams were represented by line elements placed along the center line of the members. The axial load, shear, and moment were interdependent with respect to the stability of the element. All inelastic behavior was concentrated at nonlinear hinges located at the end of the elements. These hinges had zero length and allow for plastic rotation to take place.

Masses for the model could be specified for each degree of freedom and all dynamic loads were induced by boundary accelerations. Small displacements were assumed throughout the analysis while the tangent stiffness matrix and nonlinear properties of the structure were assumed constant during each time step. All stiffness formulations were based on incremental or tangent stiffness approach.

Material Model

The beam and column elements of the frame were assumed to have a bilinear moment rotation behavior concentrated in the nonlinear hinges at the ends of the element. In the case of columns no inelastic material interaction between

the axial load and moment was assumed. The axial load had a simple elasto-plastic model for material behavior which was independent of the moment rotation behavior assumed for the bending of the element.

Due to the relative dimensions of a typical mortar joint only two stress components were used: the normal stress perpendicular to the largest dimension in the joint and the shear stress acting along the largest dimension in the joint. The assumed failure surface for the joint element is shown in Fig. 2. The joint was assumed to have linear elastic behavior up to failure. After failure only compression stresses could be carried across the joint but incremental shear stiffness relationships could exist when normal compressive stresses were present in the joint.

The wall model was assumed to be homogeneous, isotropic, and linearly elastic up to failure. The assumed failure surface for masonry is shown in Fig. 3. The surface was drawn using the principal stresses as the system of coordinates and the assumption of a plane stress condition for the masonry. Due to the inhomogeneous character of masonry the failure surface was assumed to depend on the angle that the principal stresses made with the mortar joints. To make the failure surface dependent on this angle the functional shape of the surface was assumed invariant while the five control points F_1, F_2, F_3, F_4, and F_5 were assumed to be functions of the angle. The control points F_1, F_2 depend on the principal stress angle as shown in Fig. 4. This figure is based on experimental results. The functional dependence of the control points F_3, F_4 on the principal stress angle is shown in Fig. 5. These functions are also based on experimental results which are discussed in Ref. 1. The control point F_5 was taken as the maximum of F_3 or F_4 multiplied by a constant assumed to be less than 1.

ANALYTICAL PROCEDURE

The equations of motion were stated in the incremental form assuming that the properties of the structure are constant within each time interval.

$$\begin{bmatrix} (M) & 0 \\ 0 & 0 \end{bmatrix} \begin{bmatrix} \Delta a_1 \\ \Delta a_2 \end{bmatrix} + \begin{bmatrix} (C) & 0 \\ 0 & 0 \end{bmatrix} \begin{bmatrix} \Delta v_1 \\ \Delta v_2 \end{bmatrix} + \begin{bmatrix} K_{11} & K_{12} \\ K_{21} & K_{22} \end{bmatrix} \begin{bmatrix} \Delta d_1 \\ \Delta d_2 \end{bmatrix} = \begin{bmatrix} (M) & 0 \\ 0 & 0 \end{bmatrix} \begin{bmatrix} R \\ 0 \end{bmatrix} \cdot \Delta a_g$$

where

(M) = diagonal mass matrix
(C) = damping matrix
(K_{11}) = tangent stiffness matrix for the dynamic degrees of freedom
(K_{22}) = tangent stiffness matrix for the static degrees of freedom
(K_{12}) = tangent stiffness matrix for the coupled degrees of freedom
$\{R\}$ = ground influence vector
Δa, Δv, Δd = incremental accelerations, velocities and displacement
Δa_g = incremental boundary acceleration

To integrate the equations of motion the numerical scheme developed by Newmark was used with a value of $\beta = \frac{1}{4}$. An explicit method of integration was used from which the increments in displacements may be calculated directly from the values in the previous time step. Any change in the properties of the structure during the present time interval were included as an error load vector in the next time step.

COMPUTATIONS AND RESULTS

The model proposed in the previous sections was implemented using a computer program called AWALL. Once the program was developed it was used to study a three story one bay frame infill with masonry walls. The overall dimensions of the frame are shown in Fig. 6. The structure was subjected to the El Centro ground motion of May 18, 1940, SOOE component which was scaled to 0.4g acceleration.

The properties of the frame were assumed as follows. The flexural stiffnesses were $EI_C = 31.25 \times 10^3 kN\text{-}m^2$, $EI_B = 125 \times 10^3 kN\text{-}m^2$. The yield moment was $M_y = 214.0$ kN-m. The mass per story was taken as 30 M_g while the damping ratio was taken as 2% for all modes. The modulus of elasticity for the wall was taken as 14 GPa and the thickness as 100 mm. A masonry compressive strength of 24 MPa in compression and 2.4 MPa in tension was assumed while the total wall dead load was taken as 60 kN. More detailed information is provided in Ref. 1.

Some of the results are presented in Fig. 7-12 and in Tables 1-4. Due to the complexity of the ground motion a detail discussion of all of the figures is difficult. However, there are changes in behavior that are due to a very specific event. The gap size was taken as zero for all three storys. This assumption provides two sets of frequencies at time t = 0.0. One set is based on continuity between the wall and frame, the second on the frame alone. The frequencies are shown in Table 1 and it is evident that the presence of the walls has a marked effect on the fundamental frequency of the frame. The ratio of these frequencies is about 7.5. This ratio is large enough to make a substantial difference in the earthquake forces generated on the structure. One normally uses the 1.33 Hz frequency for design; however, Fig. 7 and 8 show that the structure responds initially at the higher frequency of about 10 Hz.

Figure 7 shows the load displacement for the first story. Three main changes may be seen. The first phase is the response of the story as a frame wall system with a very high stiffness relative to the open frame. The second phase is the response of the story after cracking of the wall occurred with a lower relative stiffness. The third phase is the yielding of the columns at the base of the story giving the larger loops and permanent displacement of about 20.0 mm. These phases are summarized in Table 2 and can be observed in the relative displacement plot of Fig. 9. Figure 8 shows the load displacement for the third story. In this plot two phases may be identified. The first phase is the response of the story as a frame wall system with a very high stiffness relative to the open frame. Once the wall cracks the stiffness is reduced considerably. This may be seen in the figure. The difference between Fig. 7 and 8 is due to the lower discretization of the third story and the yielding of the columns in the first story. The change in phases of the third story are summarized in Table 4. These changes in the story stiffness may be seen in the plot of the interstory drift in Fig. 12. Although not shown the relative displacement is similar to that in Fig. 9.

Figures 10 and 11 show the time response for the second story. Little or no cracking occurred in the second story and as such its original stiffness was unchanged. Under these conditions the second story behaves as a very stiff system on top of a more flexible first story system. This is reflected in the relative displacement of Fig. 10 which is essentially the same as that of the

first story. This condition is also reflected in the interstory drift of Fig. 11 which shows a response of about 30 Hz superimposed on a slower fluctuating response. The frequency of 30 Hz is approximately the response frequency of the story if treated as a single degree of freedom system. These conditions are summarized in Table 3.

CONCLUSIONS

The proposed model seems to be able to represent the different modes of behavior observed experimentally. The crack mechanism and gap size seem to be indispensable in modeling the frame-infill-wall system and as such have a strong influence on its bahavior. The fundamental frequency of the open frame is not an adequate measure of the frequency or behavior of the system studied.

REFERENCES

1. Rivero, C.E., Walker, W.H., "An Analytical Study of the Interaction of Frames and Infill Masonry Walls", Civil Engineering Studies, Structural Research Series, No. 502, Urbana, Illinois, Sept. 1982.

Table 3 Key Response Quantities and Events: Second Story

Max. Dis. (mm)	Max. Vel. (mm/sec)	Max. Abs. Acc. (g)	Max. Res. (kN)	Max. Interstory Drift (mm)	Max. Story Acc. (g)
-36.6	-350.0	3.22	765.0	-1.39	3.62

Col.	Max. Base Mom. (kN-m)	Max. Base Shear (kN)	Min. Axial Load (kN)	Max. Axial Load (kN)
Left	76.1	38.9	70	324
Right	75.0	37.2	60	319

Summary of Key Events

Time (Sec)	Drift (mm)	Event	See Fig.
4.1	0.5	Full crack in first story detected as a change in response.	5.57
4.7	1.4	Story is very stiff compared to first story; story vibrates at a much higher frequency fluctuating about displacement of first story; frequency 30 Hz.	5.57

Table 4 Key Response Quantities and Events: Third Story

Max. Dis. (mm)	Max. Vel. (mm/sec)	Max. Abs. Acc. (g)	Max. Res. (kN)	Max. Interstory Drift (mm)	Max. Story Acc. (g)
-46.0	-497.0	-1.96	579.0	-14.8	-1.99

Col.	Max. Base Mom. (kN-m)	Max. Base Shear (kN)	Min. Axial Load (kN)	Max. Axial Load (kN)
Left	158.0	88.0	8	162
Right	162.0	90.0	-20	171

Summary of Key Events

Time (sec)	Drift (mm)	Event	See Fig.
3.5	0.1	Frame and wall act as a unit; small moments and shears; large stiffness.	5.61
4.66	1.0	Some cracking across diagonal; some change in stiffness.	5.61
5.12	1.2	Full crack across diagonal; major change in stiffness.	5.61

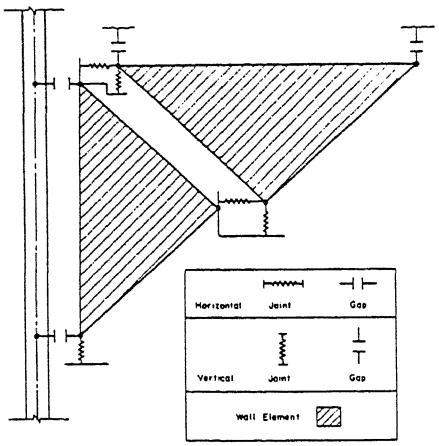

Figure 1 Schematic Representation of the Wall Model

σ_n = Normal Stress
λ_s = Shear Stress
N_t, S_i, n, m = Control Points For The Failure

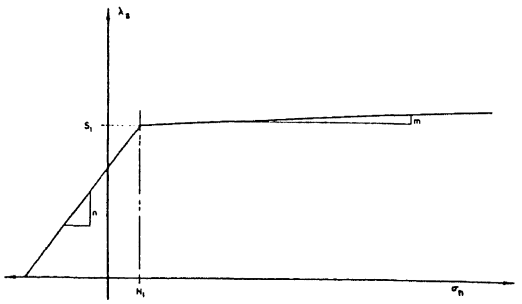

Figure 2 Joint Element Failure Surface

θ - Angle of Principal Stress with Respect to Mortar Joints

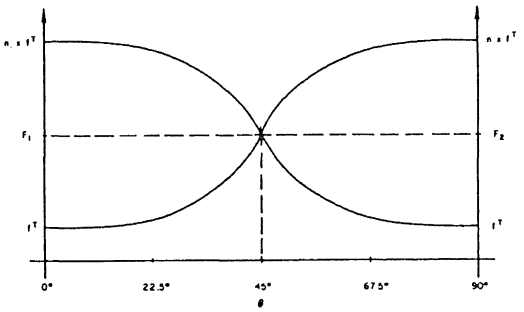

Figure 4 Uniaxial Tensile Strength of Masonry vs Angle of Principal Stress with Respect to the Mortar Joints

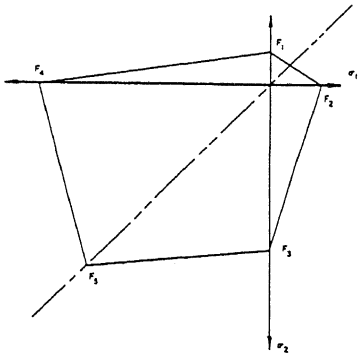

σ_1, σ_2 = Principal Stresses
F_1, F_2, F_3, F_4, F_5 = Control Points For The Failure Surface
F_5 = Max (F_3, F_4)

Figure 3 Masonry Wall Failure Surface in Principal Stresses

θ - Angle of Principal Stress with Respect to Mortar Joints

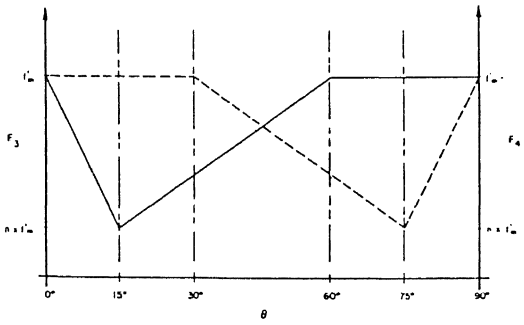

Figure 5 Uniaxial Compressive Strength of Masonry vs Angle of Principal Stress with Respect to the Mortar Joints

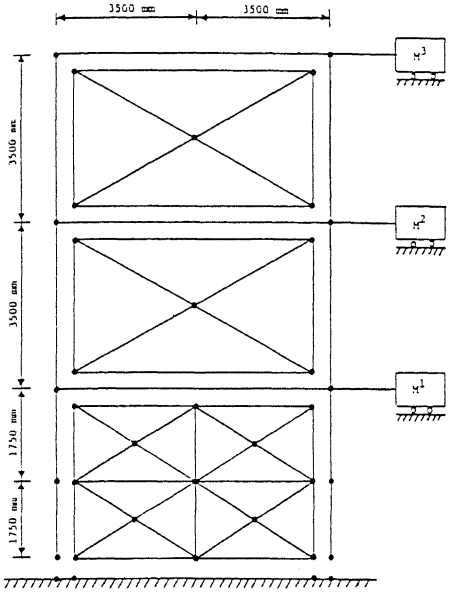

Figure 6 Overall Dimensions of the Three Story Frame

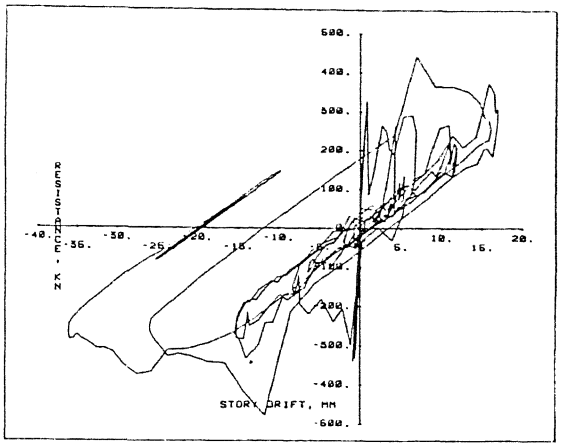

Figure 7 Load Displacement Response: First Story

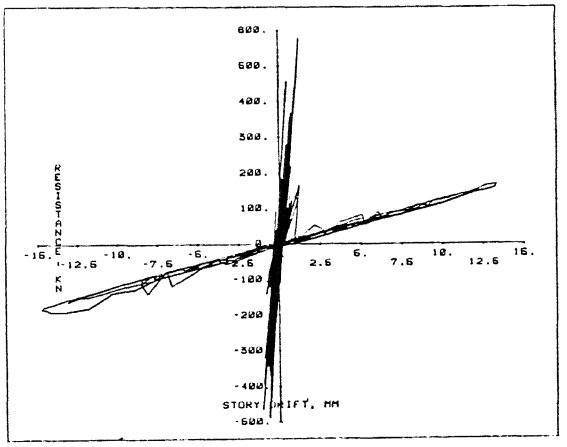

Figure 8 Load Displacement Response: Third Story

Table 1 Frequencies - Mode Shapes: Three Story Structure

	Continuous Mode No.			Gap Specified* Mode No.		
	1	2	3	1	2	3
Nat. Freq. (Hz)	9.92	32.2	54.2	1.33	4.07	6.60
Participation Factor **	8.71	3.62	-1.04	8.89	3.01	-1.41
Mode Shapes***						
Story 3	0.1473	-0.0937	-0.1138	0.1398	-0.1050	-0.0527
Story 2	0.0981	0.0787	0.1324	0.1062	0.0779	0.1264
Story 1	0.0449	0.1355	-0.0534	0.0503	0.1274	-0.1207

*Gap size = 0.

**Participation Factor = $\frac{\{q_i\}^T [M] \{R\}}{\{q_i\}^T [M] \{q_i\}}$.

***Mode shapes normalized to $\{q_i\}^T [M] \{q_i\} = 1$. $\{q_i\}$ = mode shape.

Table 2 Key Response Quantities and Events: First Story

Mag. Dis. (mm)	Max. Vel. (mm/sec)	Max. Abs. Acc. (g)	Max. Base (kN)	Max. Interstory Drift (mm)	Max. Story Acc. (g)
-36.2	-327.0	-2.75	478.0	-36.2	-2.82

Col.	Max. Base Mom. (kN-m)	Max. Base Shear (kN)	Max. Center Mom. (kN-m)	Max. Top Shear (kN)	Max. Top Mom. (kN-m)	Min. Axial Load (kN)†	Max. Axial Load (kN)†
Left	214.5	123.0	25.3	123.1	214.3	267.0	778.0
Right	214.5	123.0	69.5	162.1	214.4	233.0	796.0

Summary of Key Events

Time (sec)	Drift (mm)	Event	See Fig.
3.5	0.-0.5	Frame and wall act as a unit; large changes in axial force; small moments and shears.	5.52
4.1	0 -0.5	Full crack across diagonal of wall from top right to bottom left; large change in stiffness; moment and shears no longer small.	5.55
6.33	17.0	Frame yields at base of columns, larger loops in load displacement curve.	5.55
7.2	36.0	Max. displacement, permanent set of 20 mm.	5.56

†Axial response for bottom section of column.

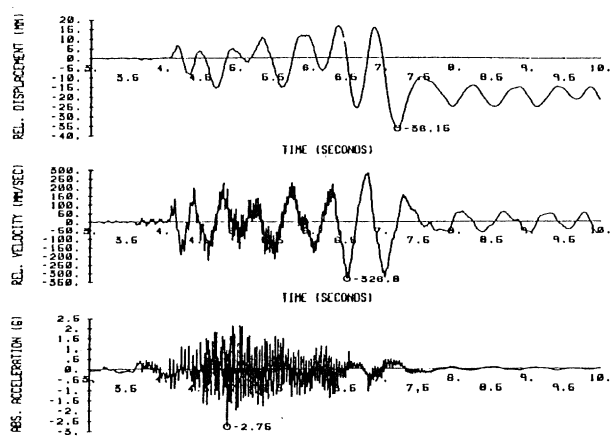

Figure 9 Relative Displacement, Velocity, and Absolute Acceleration: First Story

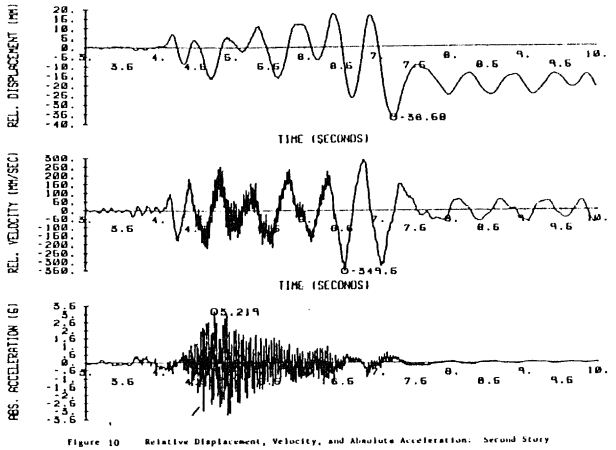

Figure 10 Relative Displacement, Velocity, and Absolute Acceleration: Second Story

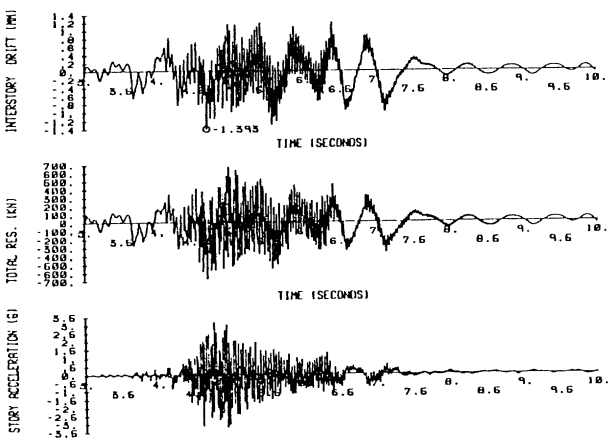

Figure 11 Interstory Drift, Total Resistance, and Story Acceleration: Second Story

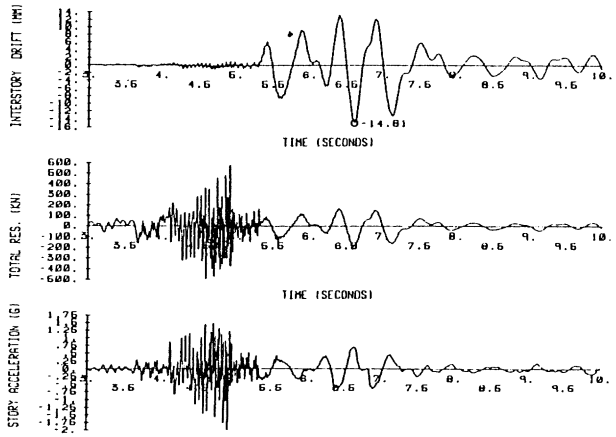

Figure 12 Interstory Drift, Total Resistance, and Story Acceleration: Third Story